DFT-Based Reaction Pathway Analysis of Hexadiene Cyclization via Carbenium Ion Intermediates: Mechanistic Study of Light Alkane Aromatization Catalysis

Yogesh V. Joshi, Aditya Bhan, and Kendall T. Thomson*

School of Chemical Engineering, Purdue University, West Lafayette, Indiana 47907

Received: July 28, 2003; In Final Form: November 4, 2003

We conducted density functional theory calculations to identify the complete cyclization mechanism (ring formation and ring expansion) for protonated hexadiene in the gas-phase as a precursory means of studying aromatization of light alkanes in acidic zeolite catalysts. We identify the rate-determining step to consist of ring expansion from a methylcyclopenta carbenium precursor to a stable cyclohexa carbenium intermediate, exhibiting an activation barrier of 9.6 kcal/mol and proceeding through a bicyclic intermediate starting from a secondary cyclopentyl carbocation. This pathway for ring closure was preferred over tertiary precursor expansion and direct cyclization to a cyclohexyl carbocation. Expecting carbocation intermediates to be represented by alkoxide species near Brønsted acid sites, we calculated the relative stability of primary, secondary, and tertiary alkoxide analogues to cyclopentyl carbocation intermediates involved in ring expansion and notice a reversal of stability relative to gas-phase carbocation stabilities (i.e., primary > secondary > tertiary stability). However, on the basis of the notion that transition state stability depends heavily on carbocation character of the transition state, even in alkoxide-based chemistry, we conclude that ring expansion would nevertheless constitute the rate-determining step in a zeolite-catalyzed mechanism.

1. Introduction

The conversion of light hydrocarbons to aromatics provides the potential for large economic gains by substantially increasing the value of liquefied petroleum gas (LPG) feedstocks. Aromatic compounds, particularly BTX (benzene, toluene, and xylene), contribute high-octane components to the gasoline pool (120+ octane value) and are important feedstock components for downstream petrochemical processing. As a consequence, over the last 50 years there has been a considerable drive to develop economically viable aromatization routes in industry.[1−5] However, aromatization catalysts suffer from a number of deficiencies. Monofunctional acid catalysts exhibit relatively low aromatics yields which is due to preferentially high cracking, isomerization, and β-scission reactivity.[6−10] Bifunctional metal/H-ZSM-5 catalysts using Ga,[11−26] Zn,[27−34] and Pt[10,7,35−40] dramatically improve aromatics yields but are prone to deactivation via coking[31] and, although better than purely acidic catalysts, are nevertheless limited in both aromatics yield and selectivity toward H_2 versus CH_4 byproducts.

The goal of ongoing research in this area is the development of highly H_2 selective catalysts for light paraffin aromatization (for reviews of this subject see the references).[20,10,41] Critical to this goal is an effort to clearly elucidate reaction pathways and mechanisms for aromatization. Aromatization of even single component feedstocks is complex, involving a large number reaction steps, many of which are not well understood or are only postulated. However, it is generally agreed that the relevant reactions for conversion of light alkanes to aromatics consists of (1) alkane C−H activation to alkoxide/carbenium complexes, (2) dehydrogenation to olefins, (3) oligomerization to higher olefins, (4) rapid isomerization, (5) β-scission, (6) cyclization, and (7) dehydrogenative aromatization.[10,41]

Cyclizations involving C(6+) olefins are believed to occur via carbocation/alkoxide-based pathways relatively independent of oligomerization.[18] Further, aromatization studies involving cyclohexane and methyl cyclohexane over Ga/H-ZSM-5 result in a very low production of light alkanes, suggesting that once naphthenic intermediates are formed they are rapidly dehydrogenated over gallium sites, forming their respective aromatic isomers.[42] Experimental investigations of carbocation chemistry, dating back to Olah's successful attempt of stabilizing carbocations in superacid solutions, exist and provide important insight into potential cyclization mechanisms.[43−46] For example, Saunders et al.[47] give experimental evidence for protonated cyclopropane intermediates for several carbocation reactions, reporting activation energies for various reactions using line shape analysis of ^{1}H NMR data. Further, there have been several experimental investigations aimed at studying the isomerization of alkylcyclopentyl cations.[48−51] However, there has not been a complete investigation of ring formation via carbocation routes specifically aimed at understanding the catalytic steps toward aromatization in acid zeolite systems.

The goal of this work was to use electronic density functional theory (DFT) calculations to investigate possible mechanisms for hexadiene cyclization via carbenium ion intermediates. We concentrated on gas-phase (noncatalytic) carbocation mechanisms in order to derive a simple theoretical baseline for modeling heterogeneous cyclization based on carbenium/alkoxide chemistry in zeolites, which is the subject of future work in our research group. Most of the previous theoretical work on ring closure mechanisms has been of gas-phase cyclization via free radical pathways[52,53] in combustion processes. For example, it was reported that the rate-determining step for soot formation is the cyclization to first benzene.[54] More detailed calculations of ring formation[52] and ring expansion[53] involving free radical intermediates have subsequently been reported. Theoretical studies of cyclization starting from C(6+) hydrocarbons are not

* Corresponding author. Phone: (765) 496−6706. FAX: (765) 494−0805. E-mail: thomsonk@purdue.edu.

10.1021/jp036205m CCC: $27.50
Published on Web 12/24/2003

SCHEME 1: Cyclization of the C_6 Diene via Carbenium Ion Intermediate, Catalyzed by Solid Acids

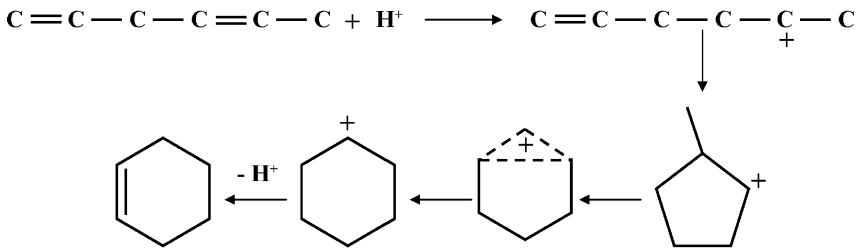

unprecedented. An MNDO study of ring expansion was reported by Viruela-Martin et al.,[55] and recently there has been a detailed study of five-membered ring expansion with relevance to sterol biosynthesis.[56] A recent ab initio study of carbenium ion reactions involved in sterol synthesis[57] also points out interesting results about ring formation. However, the precursors used for these investigations were C(8+) molecules, which contain fundamentally different alkyl groups (compared to C6 molecules) attached to the five-membered ring. It is known that aromatization of light alkanes using zeolite catalysts has high selectivity for toluene and benzene. Hence, a separate consideration for cyclization concentrating on C6 carbenium ions as precursors is desired and perhaps more relevant to zeolite chemistry. We present here details of proposed gas-phase cyclization mechanisms of hexadiene conversion to benzene based on carbenium ion chemistry. This work represents the first step in understanding cyclization mechanisms in zeolite catalysts, the subject of future investigations in our group.

This rest of this paper is organized as follows. Section 2 describes the particulars of our hypothesized cyclization mechanism, providing the rationale for this study. In section 3 we describe the computational details of our calculations. In section 4 we present the results of our calculations, laying out the mechanisms for different parts of the cyclization and presenting the energetic analysis of intermediates and transition states for the following components/steps: (4.1) precursor geometries, (4.2) activation of the precursor, (4.3) ring formation, (4.4) hydride transfer, (4.5) ring expansion, and (4.6) direct cyclization as an alternative mechanism. In section 5 we present a discussion of the results, concentrating on how our calculations likely translate to catalytic mechanisms in ZSM-5. In section 6 we provide a summary of our conclusions.

2. Cyclization Mechanism

Experimental elucidation of catalytic cyclization mechanisms is challenging and problematic. Difficulties include (i) the inability of experimental detection of various intermediates involved in cyclization and (ii) the possibility of multiple intermediates, which makes it very difficult to suggest a reasonable sequence of the elementary steps and even more difficult to quantify and partition the energetics. Hence, the use of molecular DFT simulations to propose and verify reaction mechanisms is well suited for this system. Coupled with full transition state searches, these calculations can provide important information about relative reaction rates, which is useful in identifying rate-limiting steps and the effect of microstructural aspects of the catalyst on reaction rates.

With the help of the carbenium ion chemistry, a sequence of elementary steps was proposed as shown in Scheme 1.[41,20] The various dienes generated through oligomerization are assumed to be precursors for cyclization. In this scheme these dienes accept protons to first form reactive carbenium ions. Cyclization is presumed to occur as the non-carbocationic unsaturated double bond attacks the positive cationic charge center, closing the ring. The resulting alkylcyclopenta carbenium ions can then undergo a series of hydride transfers to form stable tertiary carbenium ions, which subsequently undergoe ring expansion to form the cyclohexa carbenium ion.

In the catalytic cyclization route, the carbenium ion intermediates are assumed to reside in the vicinity of active Brønsted sites, possibly as stabilized alkoxide compounds. However, we felt it was useful to first study gas-phase carbenium ion cyclization mechanisms, as this will provide a basis for hypothesizing catalytic routes. We will eventually verify the kinetic feasibility of similar elementary steps involved in zeolite-catalyzed cyclization. We will use the resulting intermediate geometries as starting guesses for full DFT studies involving embedded cluster models of zeolite sites.

3. Computational Methods

All calculations were carried out using the B3LYP hybrid density functional[58] with a 6-311+G(2d,p) basis set for all atoms.[59] All structures were optimized to tight convergence criteria using the GAUSSIAN 98 commercial code.[60] We believe this choice of functional and basis set is the best for the type of system we are investigating. In its original formulation the parameters in the B3LYP functional were determined by least-squares fitting to the G2 set of atomic and molecular energy data. Almost half of this set is related to ionization energies of various atoms and molecules. We also opted for the MP2 optimized 6-311+G(2d,p) single-ζ core, triple-ζ valance basis sets, which are known to outperform basis sets optimized at the Hartree−Fock level[61] for non-HF calculations. Transition states (TS) were calculated using a quadratic synchronous transit algorithm (QST).[62] Initial guesses for TS searches were generated in several ways. In general, the midpoint along the linear synchronous transit (LST) path was used as the initial guess for the QST optimization. However, more complex reaction paths were analyzed by QST path optimization first. These path calculations were mainly used to generate more accurate guesses. The energies reported here have not been corrected for zero-point vibration energies. Because all reaction paths under consideration involve rearrangement of the atoms in different conformers, the magnitude of the basis-set-superposition error (BSSE) should be very small and was ignored.

We conducted our pathway analysis by considering the already protonated 1,4-dihexene ($C_6H_{11}^+$, IUPAC: hex-5-en-2-ylium). Protonation and de-protonation of the cationic reactant and product were not studied, and all energies are reported relative to the most stable acyclic conformer of $C_6H_{11}^+$ found; this initial reactant molecule ($C_6H_{11}^+$) has a complex potential energy surface (PES) involving several local minima, and at least 12 stable minima (including cyclic intermediates) were located at the above-mentioned level of theory. Most of the structures we report along the reaction path were the direct result of intermediates postulated according to classical carbenium ion

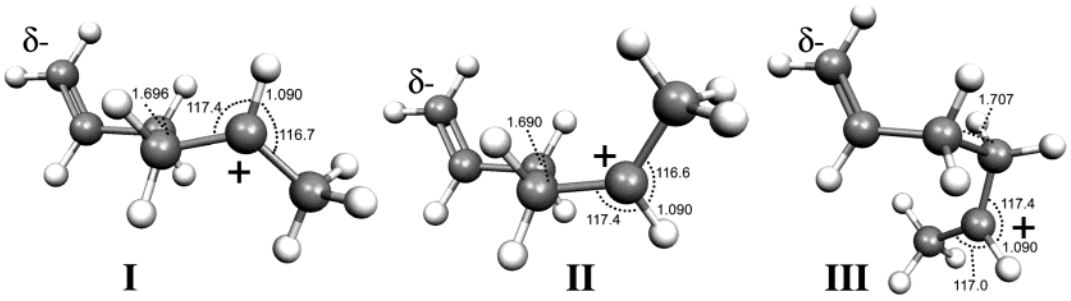

Figure 1. Three of the five acyclic conformers acting as precursors for cyclization.

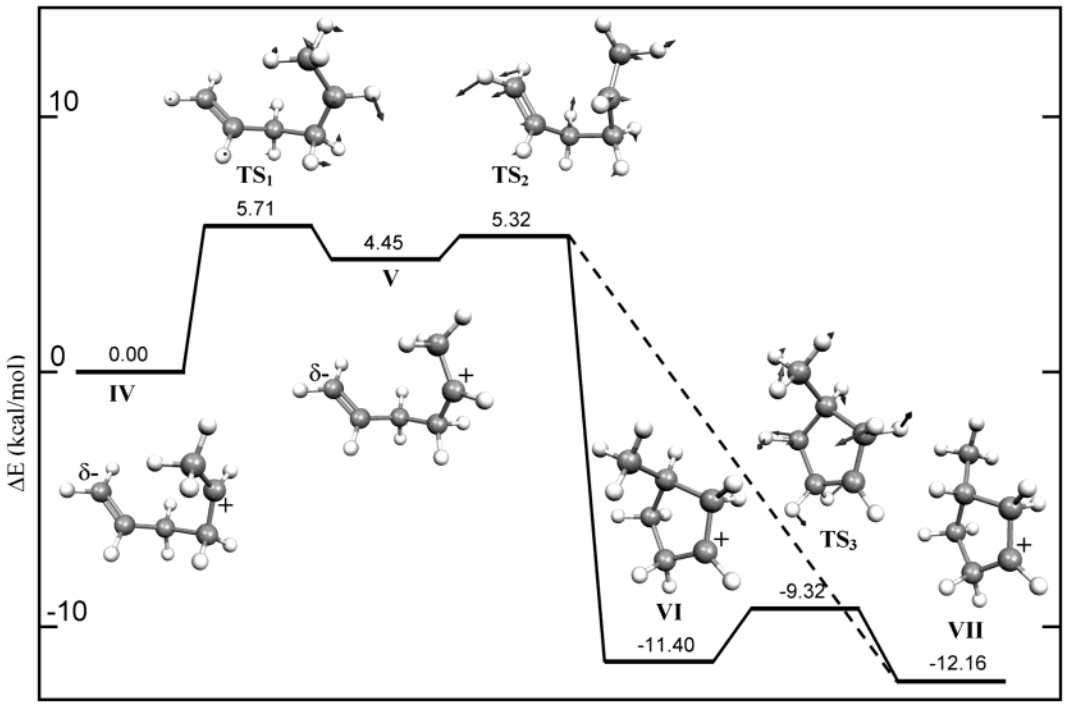

Figure 2. Reaction pathway for precursor activation and ring formation of the carbenium ion (IUPAC: hex-5-en-2-ylium). Energies are in kcal/mol.

chemistry. Additional transition states with aberrant imaginary vibration modes were tested for stable reactants and products on the reaction path. These also gave rise to additional stable intermediate conformers.

4. Results

4.1. Precursor Geometries. At the level of theory under consideration, we found five stable acyclic conformers (designated I, II, III, IV, V in Figures 1 and 2) for the $C_6H_{11}^+$ precursor cation. Of these conformers structures I and II are more linear in configuration compared to the other three.

We conducted a Mulliken charge analysis (see Table 1) on each of these structures and show that all of these acyclic conformers can be characterized by two main charge centers: (1) a substantial positive charge center (+) at the cation position and (2) a negative charge center ($\delta-$) at the terminal atom of the non-protonated double bond. One would expect that the electron rich terminal carbon ($\delta-$) should attack the electrophilic positive charge center (+), giving rise to a methylcyclopenta carbenium ion (structure VI) as shown in Figure 2. On the basis of this consideration, we would expect the most reactive precursor conformer to exhibit the greatest charge difference among charge centers (from + to $\delta-$), which would make the electrophilic attack more viable. Of the five conformers, structure V exhibits the greatest charge difference, whereas conformer IV (the most stable conformer) has a substantially lower value. As can be seen in Table 1, it is the carbocation charge that is most important, as the terminal carbon charge $\delta-$ is relatively unchanging among conformers.

4.2. Activation of the Precursors. On the basis of these observations, we chose a representative pathway consisting of the lowest energy precursor (IV) undergoing activation by a change in conformation to intermediate V, which subsequently undergoes ring formation as described in the next section. Although we acknowledge that several consistent pathways involving all five conformers ultimately undergoing ring formation exist, we nevertheless chose this representative possibility as a means of characterizing the most probable energy route to cyclization. The transition state for this activation is shown in the Figure 2 by structure TS_1, and the eigenvector corresponding to the reaction coordinate is indicated with arrows. Transition states for interconversion between other precursor conformers are assumed to be irrelevant.

4.3. Ring Formation. As explained in section 4.1, ring formation occurs as the electron rich terminal carbon ($\delta-$) attacks the positively charged carbenium center, in this case giving rise to a methylcyclopenta carbenium ion (IUPAC: 3-methylcyclopent-1-ylium) as shown by structures VI or VII in Figure 2. The presence of the tertiary branched carbon in the cyclic product makes it more stable compared to any acyclic

TABLE 1: Relative Energies of Carbenium Ion Intermediates and Transition States (TS)

	total energy (Hartree)	relative energy (kcal/mol)	charge at carbocation position[a,b]	charge at electron rich carbon[a]	difference
I	−234.99953725	0.8723	0.307	−0.2600	0.5670
II	−234.99948329	0.9062	0.350	−0.2640	0.6140
III	−234.99819200	1.7165	0.354	−0.2760	0.6300
IV	−235.00092739	0.0000	0.340	−0.2580	0.5980
V	−234.99383955	4.4477	0.413	−0.2700	0.6830
VI	−235.01908875	−11.3964	0.247		
VII	−235.02029766	−12.1550	0.292		
VIII	−235.02159488	−12.9690	0.209		
IX[d]	−235.023487152	−14.1565			
X	−235.04515157	−27.7511	0.751		
XI	−235.02153580	−12.9320	0.257		
XII	−235.02544054	−15.3822	0.336		
XIII	−235.02773504	−16.8221	0.350		
TS_1	−234.99183219	5.7073	0.385		
TS_2	−234.99218594	5.3228	0.360		
TS_3	−235.01578249	−9.3217	0.371		
TS_4	−235.01445996	−8.4918	0.149[c]		
TS_5	−235.0169804	−10.0734	0.222[c]		
TS_6	−235.0154175	−9.0927	0.208[c]		
TS_7	−234.9884933	7.8025	0.248[c]		
TS_8	−235.0202777	−12.1425	0.389		
TS_9	−235.0062368	−3.3317	0.186		
TS_{10}	−234.9667312	21.4585	0.016		

[a] Mulliken charge. [b] For transition states, the highest positive charge on any carbon. [c] The tertiary carbon assumes higher positive charge than any other carbon. [d] This structure is not stable at strict convergence criteria for geometry optimization.

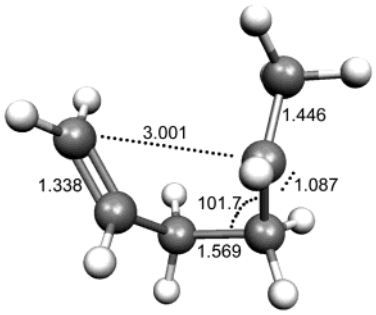

Figure 3. Transition state for the ring formation step in the cyclization mechanism. Arrows indicate the vibration mode corresponding to the reaction coordinate.

precursor (see Table 1). This is because the tertiary carbon in the ring stabilizes the secondary carbocation, even though it is not in immediate proximity. We see this directly by observing that the tertiary carbon has a significant positive charge compared to the rest of the neutral (valance satisfied) carbons in the structure. This also agrees with the popular notion that branched carbocation isomers are energetically more stable than linear ones.

For this cation, we observed two methylcyclopenta carbenium conformers (designated VI and VII). Structure VI is characteristically nonplanar as the methyl group is out of the plane of the 5-fold ring. By contrast, structure VII has its methyl group almost in the plane. We observe the nonplanar structure (VI) to be slightly more stable than the planar structure.

The transition state for ring formation is shown as structure TS_2 in the Figures 2 and 3. The vibrational mode (in Figure 2) clearly corresponds to relative motion between the positive and negative charge centers (ring formation). Because the transition state structure is very similar to the reactant in character, it was difficult for us to trace the entire path from the transition state to both of the product geometries VI and VII. However, we speculate that pathways to both products exist that have very similar activation energies and relatively analogous transition state geometries. It is interesting to note that the actual cyclization step has a very small activation energy, which is consistent with our expectations of high reactivity due to the large difference between charge centers in structure V. Jenson and Jorgensen[57] even report unactivated 1−5 ring closure starting from a *tertiary* precursor to form a tertiary cyclopentyl cation. Hence, we believe 1−5 ring closure to be effectively a weakly activated process in general.

4.4. Hydride Transfer. The transition state for interconversion between conformers VI and VII was also calculated and is shown in Figure 2 (as TS_3). The activation barrier is relatively small and suggests fairly rapid equilibration. In addition, both structures are also susceptible to hydride transfer steps, which we observe to be of comparable activation energy to that of conformer equilibration.

Before ring expansion can occur, the carbocation center must migrate around the ring to form a carbocation structure more conducive to ring expansion. The most obvious stable cation is in the tertiary position (conformer X). We observed that both structures VI and VII undergo hydride transfer to produce the tertiary carbenium ion. The calculated reaction path for structures VI and VII are shown as "path 1" and "path 2" in Figure 4. The transformation to a tertiary carbenium ion occurs through two consecutive hydride transfer steps.

Because we observed the tertiary carbenium ion (X) to have a planar geometry, with the methyl group lying nearly in the 5-fold ring plane, we expect the planar conformer VII to have a more direct reaction path to X. This is shown in Figure 4, where the pathway for structure VI undergoes an additional reorientation (XIII → IX) from a nonplanar secondary cation to a more planar structure prior to the final hydride transfer.

We found that the secondary cation IX was unstable at the current level of theory and tight convergence criteria and accordingly relaxed (unactivated) to the low energy tertiary carbenium ion directly. The reason this reaction is so fast is because of the structural similarity between the planar conformer of structure IX and the sp^2 hybrid tertiary carbon in structure X. The fact that a tight convergence criterion renders structure IX unstable indicates either a very shallow minima or an inflection point on the PES corresponding to this conformer.

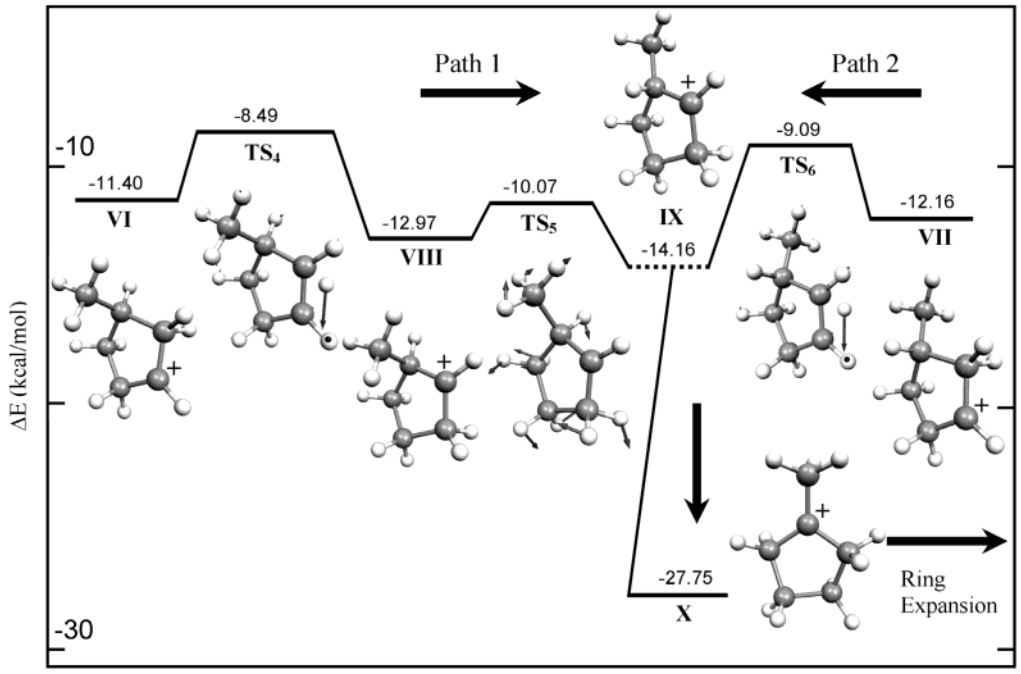

Figure 4. Reaction pathway for hydride transfer leading to the formation of the tertiary carbenium ion (IUPAC: 3-methylcyclopent-1-ylium). Energies are in kcal/mol.

SCHEME 2: Proposed Pathways for Ring Expansion[a]

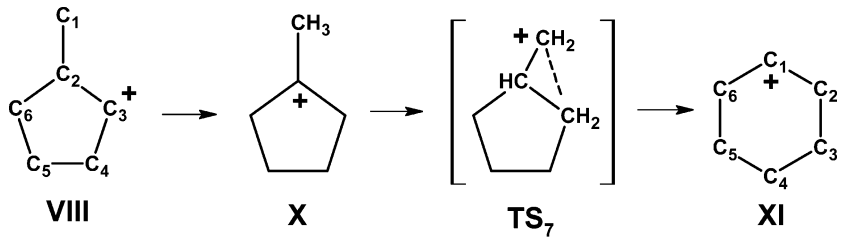

Pathway 1

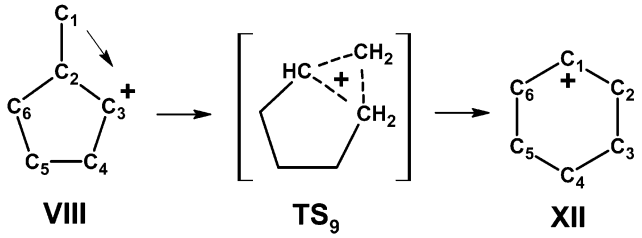

Pathway 2

[a]Pathway 1 corresponds to expansion via a tertiary cyclopentyl precursor. Pathway 2 corresponds to expansion via a secondary cyclopentyl precursor through a bicyclic cyclohexylium transition state

The reported energy and geometry is for the structure we calculated with the least root mean square (rms) value of the forces, which is well below the regular convergence criterion of GAUSSIAN 98.

The transition state for the hydride transfer reaction between VI and VIII is shown in Figure 4 as TS_4. A similar transition state for hydride transfer between VII and IX is shown in Figure 4 as TS_6. Both transition states are comparable in structure and have nearly identical activation energies. Our results agree with experimental[51] reports of activation energies in a similar range (~3 kcal/mol) for alkyl cyclopentyl carbenium ions. An extensive transition state search between structures VIII and X resulted in the transition state indicated by structure TS_5 in Figure 4. A close examination of the geometry of TS_5 and of the reaction coordinate eigenvector indicates that conformer VIII tends to become planar to form the structure IX before proceeding downhill to the tertiary cation X.

4.5. Ring Expansion. Several investigations report multiple ring expansion pathways from cyclopentyl carbocations.[47,56,57,63] In a theoretical analysis of the isopropylcyclopentyl carbenium ion, Vrcek et al.[56] report three such pathways. However, the probability of different pathways depended on the precursor for ring expansion. They found that starting with a cyclopentyl precursor with a larger alkyl side chain (like isopropyl), they observe stable intermediates with carbocation centers situated on carbons that are not part of the cyclopentyl ring. For the

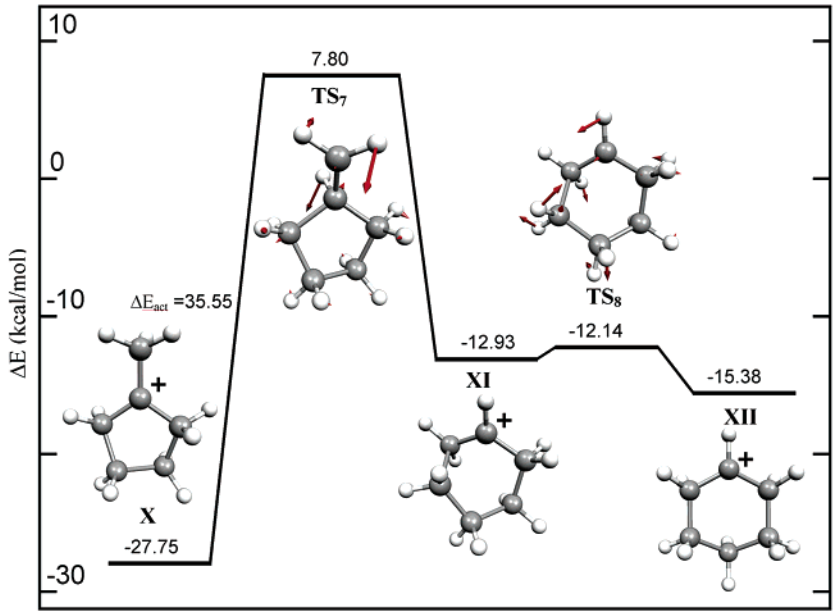

Figure 5. Reaction pathway 1 for ring expansion of tertiary carbenium ion to cyclohexa carbenium ion (IUPAC: cyclohexylium). Energies are in kcal/mol.

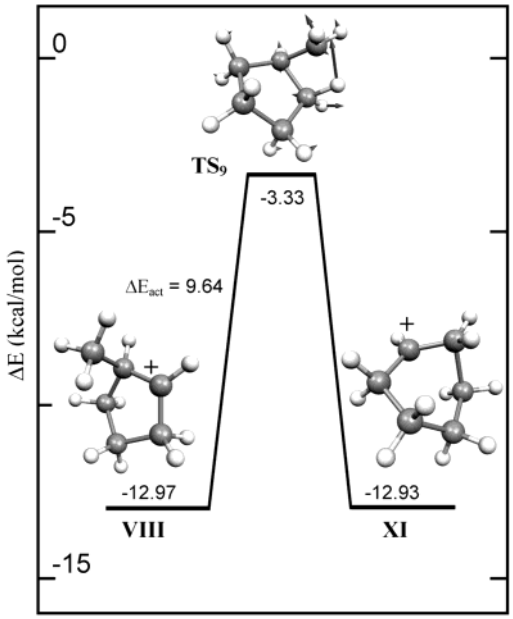

Figure 6. Reaction pathway 2 for ring expansion of secondary methylcyclopentyl carbenium ion to cyclohexyl carbenium ion (IUPAC: cyclohexylium). Energies are in kcal/mol.

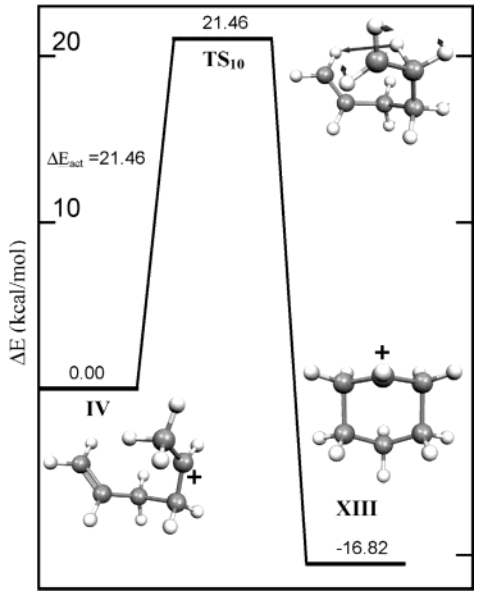

Figure 7. Reaction pathway for direct cyclization of the secondary carbenium ion to a cyclic carbenium ion (IUPAC: cyclohexylium). Energies are in kcal/mol.

case we are investigating (methylcyclopentyl cation precursor), this seems unlikely as it would result in a primary carbocation.

We found two mechanistically feasible paths for ring expansion, involving either the tertiary precursor X (pathway 1) or the secondary precursor VIII (pathway 2) as shown in Scheme 2. In the first pathway, ring expansion starts with a hydride transfer from the terminal methyl group to the tertiary carbenium center (see Figure 5). Simultaneously, the bond between C2 and C3 is broken. Consequently, C1 forms a bond with C3 to give a cyclohexa carbenium ion. For the resulting six-membered cyclic carbenium ion, we observed at least three conformers. They are shown as structures XI, XII (in Figure 5), and XIII (in Figure 7). The geometry of structure XI is such that the carbocation atom is well out of the plane, forming a bicyclic intermediate, with the cation charge ostensibly shared among three carbons (C1, C2, C3) all nearly equidistant to one another (as portrayed in Scheme 1). A Mulliken charge analysis shows the charge is predominantly situated on the C2 carbon.

The transition state for pathway 1 is shown as structure TS_7 in Figure 5 and Figure 8a. The eigenvector corresponding to the reaction coordinate is indicated with arrows. This vibration mode clearly indicates the stretching of the C2−C3 bond with simultaneous hydride transfer. We calculated an activation energy of 35.55 kcal/mol for this step, which reflects both the large stability of the tertiary carbocation, and the fact that the transition state has partial *primary* carbenium ion character. After formation of the six-membered intermediate XI, the carbocation stabilizes through transformation to a more planar and symmetric structure (XI). The corresponding transition state for this transformation is shown in Figure 5 as TS_8.

The second pathway for ring expansion starts from VIII, the secondary cation structure, and proceeds via a hydride transfer from the methyl group to the secondary charge center (see Figure

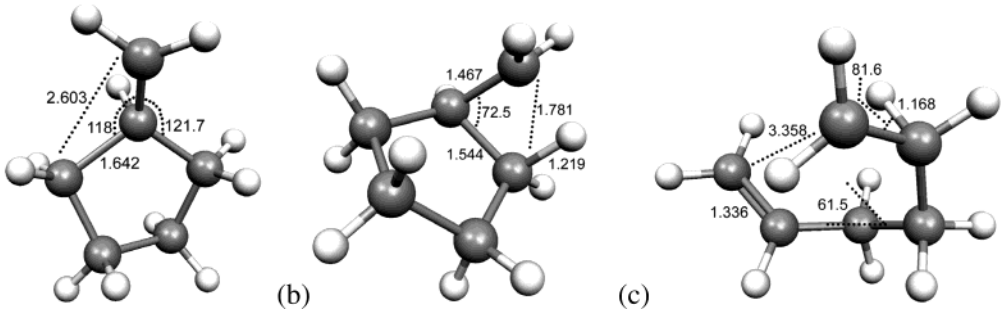

Figure 8. Critical transition state geometries for (a) ring expansion pathway 1 (TS_7), (b) ring expansion pathway 2 (TS_9), and (c) direct cyclization (TS_{10}).

6). This occurs simultaneously with breaking of the cyclopentyl bond to form a cyclohexyl structure, which stabilizes the resulting primary charge center on the methyl group. We observed the transition state for this path to be much lower in energy compared to "pathway 1", and hence, "pathway 2" is much less activated. The transition state geometry resembles a bicyclohexilium ion analogous to that observed by Vrcek et al.[56] in a proposed mechanism for isopropylcyclopentane ring enlargement (pathway III of Scheme 2 in their article). They report an additional symmetric intermediate which is stable at the MP2/6-31G(d) level but is located at a transition state in the B3LYP/6-31G(d) level. Using B3LYP, we find our structure (TS_9) to be a transition state, and no stable intermediate was found. It is unknown whether this was simply an artifact of the DFT method, as Vrcek et al. used the more accurate Møller−Plesset perturbation methods, or whether such intermediates are truly precluded in this particular system. As an argument for the later, we expect the resulting carbocation center on the methyl group (in the methylcyclopentyl carbenium system) would make such a structure less stable compared to that in the isopropylcyclopentyl carbenium system studied by Vrcek et al. The C2−C3 isopropyl shift must be less activated compared to the C2−C3 methyl shift. Hence, we see a higher activation barrier (∼9.6 kcal/mol) for ring expansion of the methyl cyclopentyl carbenium ion than Vrcek et al. saw for the isopropyl carbenium ion (∼4.2 kcal/mol).[56]

4.6. Direct Cyclization (1,6 Ring Closure). For completeness, we also considered the possibility of direct cyclization via 1,6 ring closure (without formation of a cyclopentyl intermediate). We found that direct cyclization occurs via the following simultaneous events: (i) hydride transfer from the terminal β-carbon to the secondary carbenium center and (ii) bond formation between the β-carbon and the other terminal carbon leading to cyclization. The relevant geometries and energetics for direct cyclization of conformer IV are shown in Figure 7. We report an activation energy for this route of 21.46 kcal/mol.

5. Discussion

On the basis of our analysis, we find that the most energetically favorable route for C6 cyclization involves first ring closure to a stable cyclopenta carbenium intermediate, followed by ring expansion through a secondary (bicyclic) carbenium precursor (pathway 2 in Scheme 2). The overall change in energy for this route is −15.3 kcal/mol. We identify the rate-determining step to be ring expansion, with a calculated activation energy of 9.6 kcal/mol. Both direct cyclization and ring expansion via a tertiary cyclopentyl precursor had markedly higher activation energies (21.5 and 35.6 kcal/mol, respectively) and do not seem likely as gas-phase cyclization routes.

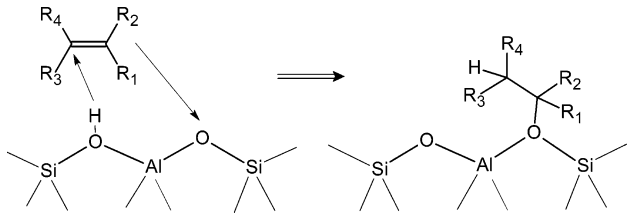

Figure 9. An alkene chemisorption process to form an alkoxide-like intermediate.

The reason for this ordering of activation energies becomes clear when we compare the critical transition states (the TS representing the most activated step) for each reaction pathways. Figure 8 shows the critical transition state geometries. Both transition states a and c exhibit partial *primary* carbocation character, leading to relatively high activation energies (i.e., low stability at the transition state). However, for the bicyclic TS b, the carbocation charge center is shared among three carbon atoms, exhibiting effectively *secondary* carbocation character. Also TS b truly represents the concerted reaction path where several reaction steps (like C1−C3 hydride transfer, C2−C3 bond scission, C1−C3 bond formation) occur simultaneously. As mentioned before, although we were unable to form a stabilized bicyclohexilium ion as an intermediate, stable bicyclohexilium intermediates were observed computationally for analogous systems, with side chain groups commensurate with more stable carbocation character. Hence, we expect the activation barrier for ring expansion to decrease as we move from methylcyclopentyl to ethylcyclopentyl to isopropylcyclopentyl. We expect C6 ring formation to be slower than C(7+) in general, provided steric factors of the zeolite cage do not interfere (for aromatics > C_7, shape selectivity and the cracking activity of zeolites should control the selectivity). This observation also explains the observed higher selectivity for toluene as an aromatic fraction.

It should be noted that the tertiary methylcyclopentyl carbenium intermediate does not lie on the shortest and least activated path for cyclization. The only way it could affect the cyclization is through its stability. One should expect the tertiary methylcyclopentyl carbenium intermediate to populate most of the carbenium ion pool, and in that case the ring expansion by pathway 1 might be significant.

We are now in a position to discuss how these gas-phase calculations will correlate with zeolite-catalyzed cyclization pathways. Over the past decade many theoretical investigations have been carried out for zeolite-catalyzed hydrocarbon processing.[64−69] On the basis of these studies it is generally believed that, although zeolites show very high acidity, chemisorbed (protonated) alkenes form alkoxide bonds with bridging oxygen atoms, rather than exist as formal carbocations. Consequently, primary, secondary, and tertiary alkoxide stability

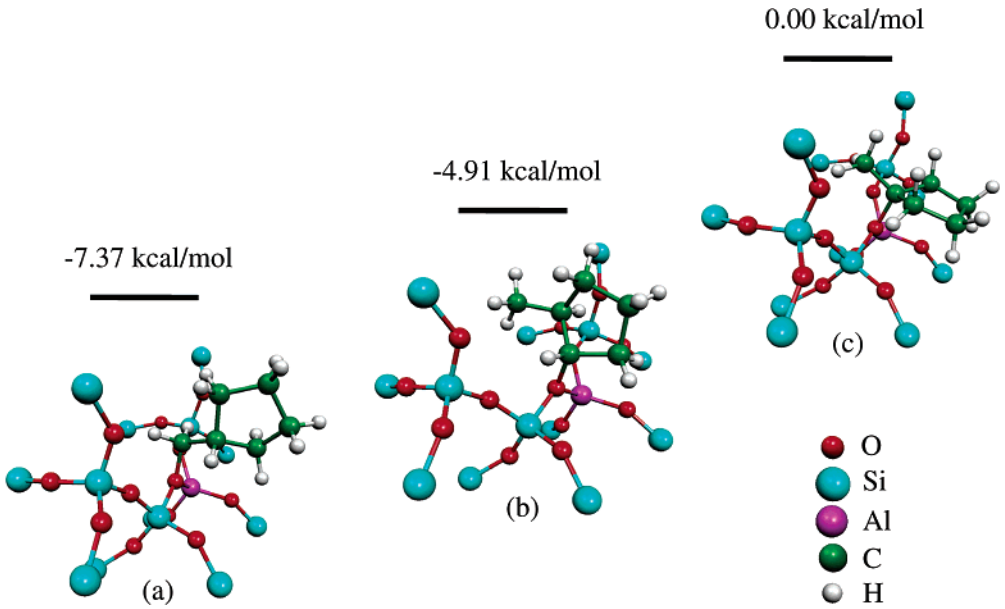

Figure 10. Various intermediates for cyclization on a Brønsted acid site: (a) primary alkoxide; (b) secondary alkoxide; (c) tertiary alkoxide.

does not simply follow the rules for solution/gas-phase carbenium chemistry. Hence, we expect that the intermediate carbocation structures observed in our gas-phase mechanism would translate to their alkoxide counterparts in the zeolite-catalyzed mechanism.

To test this, we studied the stability of key cyclopentyl intermediates using a cluster model representation of the T12 Brønsted acid site on H-ZSM-5. A representative zeolite cluster for these calculations was prepared from crystallographic data published by Koningweld et al.[70] The cluster was terminated by SiH_3 groups with Si−H distances fixed at 1.498 Å. All terminal Si and H atom positions were frozen in these calculations, and silicon at the T12 position was replaced by Al to represent the conjugate base of the Brønsted acid site, which included a charge-compensating proton near the Si−O−Al bridging oxygen. All calculations were conducted at the B3LYP/6-31G(d,p) level of theory, and full relaxation of all nonfrozen atoms was obtained. In the fully relaxed structures, Al−O bond lengths were slightly larger compared to the crystallographic lengths for Si−O as expected. This expansion is compensated by rotation of surrounding Si coordination tetrahedra. It has been shown previously that unsaturated hydrocarbons accept the proton from a Brønsted acid site at the C−C double bond. The other carbon from the double bond subsequently binds to the oxygen from the conjugate Brønsted base forming an alkoxide-like intermediate. This process is schematically presented in Figure 9.

Relaxed geometries and energies for three methylcyclopentyl structures forming primary, secondary, and tertiary alkoxide species are shown in Figure 10. Comparing the energies of each alkoxide, we observe the order of relative stability to be completely reversed from the analogous gas-phase stability of the corresponding carbocations, for which the stability order is 3° > 2° > 1°.

To explore this further we compared alkoxide species with analogous gas-phase methyl cyclopentyl molecules, where we replaced the alkoxide conjugate base (represented as −OZ) with −OH (alcohol), −Cl, and −F (halides). Figure 11 gives a schematic of the compounds and Table 2 presents a comparison of the relevant bond characteristics. As with the alkoxide compounds, all gas-phase molecules were fully relaxed at the B3LYP/6-31G(d,p) level. We see that although the C−X charge

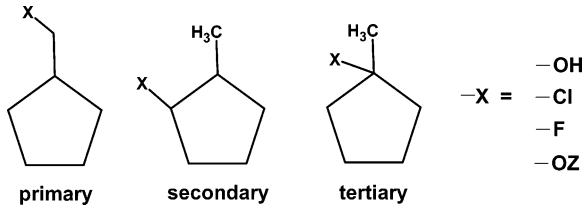

Figure 11. Gas-phase species studied for comparison of their C−X bonding properties with those of C−OZ (representing adsorbed alkoxide on zeolite, Z) that are tabulated in Table 2.

TABLE 2: Key Parameters for Carbenium Ion Pairing with Several Conjugate Bases

conjugate base		relative energy[a]	C charge[b]	O charge[b]	C−O bond length[c]
zeolite site	primary	0.0000	0.0223	−0.6636	1.5156
	secondary	2.4679	0.1468	−0.6734	1.5313
	tertiary	7.3738	0.2584	−0.7078	1.6203
OH^-	primary	0.0000	−0.1417	−0.4154	1.4447
	secondary	−2.8913	0.0643	−0.4250	1.4229
	tertiary	−4.9700	0.4510	−0.4671	1.4277
Cl^-	primary	0.0000	−0.4806	−0.0165	1.8272
	secondary	−2.1652	0.3686	−0.1815	1.8254
	tertiary	−3.3071	1.0622	−0.4555	1.8709
F^-	primary	0.0000	−0.1310	−0.2988	1.4061
	secondary	−3.8143	0.0841	−0.3184	1.4166
	tertiary	−7.2610	0.5179	−0.3486	1.4308

[a] In kcal/mol. [b] Mulliken charge. [c] In angstroms.

polarities increased in the sequence 1° → 2° → 3° in all cases, the relative stabilities of the alcohol and halide molecules were opposite of the observed alkoxide order (agreeing instead with the relative stability of carbocations). Hence, we believe interactions of adsorbed alkoxide with the surrounding zeolite lattice play a governing role in determining alkoxide stability in zeolite pores. We expect nominally that alkoxide stability would order as the corresponding alcohol/carbocation stability, yet because each alkoxide leads to structurally different environments when bonded at a Brønsted site, zeolite−alkoxide interactions override this order.

If we can assume that directly analogous reaction routes for cyclization occur in the zeolite-catalyzed mechanism, then we still expect the most likely path for cyclization proceeds through

pathway 2, with the bicyclic TS. Although we cannot necessarily predict the stability of the alkoxide intermediates along these pathways, we can conclude that the relative activation energies for different pathways will still be governed by gas-phase carbocation relative stability. This in fact has been observed by several investigators who show that although primary versus secondary alkoxide stability near Brønsted acid sites does not follow gas-phase carbocation rules, transition states for formation of these alkoxide exhibit strong carbocation character, and consequently activation energies do correlate appropriately. What remains to be seen is whether steric factors govern cyclization pathways by inhibiting the formation of transition states through repulsive interactions with the zeolite cage. These questions are the subject of ongoing work in our research group.

6. Conclusions

We have conducted DFT calculations to analyze and test plausible reaction pathways for C6 cyclization via gas-phase carbocation routes. On the basis of the analysis of the pathway energetics, we find a rate-determining activation barrier of 9.6 kcal/mol, corresponding to ring expansion from a cyclopentyl precursor to a cyclohexyl stable intermediate. This reaction step proceeds through a bicyclic intermediate starting from a secondary cyclopentyl carbocation, which was preferred over tertiary precursor expansion and direct cyclization pathways.

We expect that this reported mechanism will translate qualitatively to the case of cyclization via zeolite-catalyzed routes, and ongoing research is being conducted in this area. The most notable difference we expect is the relative stability of alkoxide-based intermediates in the zeolite versus gas-phase carbocation stability. On the basis of previous calculations of alkoxide formation through protonation, which report activation barriers on the order of 18 kcal/mol,[69] we propose that cyclization is not rate determining in the full aromatization reaction network. However, a full reaction pathway analysis incorporating Brønsted acidity near a zeolite site is needed before a firm conclusion can be made.

Acknowledgment. This work was supported by the State of Indiana through a Grant from the 21st Century Technology Fund and through the National Science Foundation GrantNo. CTS-0238989-CAREER. Computational resources were obtained through a Grant from the National Computational Science Alliance (AAB proposal No. ESC030001) and through supercomputing resources at Purdue University.

Supporting Information Available: Structures, bond lengths, bond angles, and Mulliken charges for I−XIII, TS1−10, and Figure 10a−c. This material is available free of charge via the Internet at http://pubs.acs.org.

References and Notes

(1) Mowry, J. R.; Martindale, D. C.; Hall, A. H. P. *Arabian J. Sci. Eng.* **1985**, *10*, 367−375.
(2) Mowry, J. R.; Anderson, R. F.; Johnson, J. A. *Oil Gas J.* **1985**, *83*, 128−131.
(3) Doolan, P. C.; Pujado, P. R. *Hydrocarbon Process.* **1989**, *68*, 72.
(4) Chen, N. Y.; Garwood, W. E.; Dwyer, F. G. *Shape Selective Catalysis in Industrial Applications*; Marcel Dekker: New York, 1996; Vol. 65.
(5) Chen, N. Y.; Yan, T. Y. *Ind. Eng. Chem. Process Des. Dev.* **1986**, *25*, 151−155.
(6) Anderson, J. R.; Foger, K.; Mole, T.; Rajadhyaksha, R. A.; Sanders, J. V. *J. Catal.* **1979**, *58*, 114−130.
(7) Dass, D. V.; Odell, A. L. *J. Catal.* **1988**, *113*, 259−262.
(8) Shigeishi, R.; Garforth, A.; Harris, I.; Dwyer, J. *J. Catal.* **1991**, *130*, 423−439.
(9) Ono, Y.; Kanae, K. *J. Chem. Soc., Faraday Trans.* **1991**, *87*, 663−667.
(10) Guisnet, M.; Gnep, N. S.; Aittaleb, D.; Doyemet, Y. J. *Appl. Catal., A* **1992**, *87*, 255−270.
(11) Chen, N. Y.; Garwood, W. E.; Heck, R. H. *Ind. Eng. Chem. Res.* **1987**, *26*, 706−711.
(12) Kitagawa, H.; Sendoda, Y.; Ono, Y. *J. Catal.* **1986**, *101*, 12−18.
(13) Gnep, N. S.; Doyemet, J. Y.; Seco, A. M.; Ribeiro, F. R.; Guisnet, M. *Appl. Catal.* **1988**, *43*, 155−166.
(14) Gnep, N. S.; Doyemet, J. Y.; Guisnet, M. *J. Mol. Catal.* **1988**, *45*, 281−284.
(15) Price, G. L.; Kanazirev, V. *J. Catal.* **1990**, *126*, 267−278.
(16) Mao, R. L. V.; Carli, R.; Yao, J. H.; Ragaini, V. *Catal. Lett.* **1992**, *16*, 43−52.
(17) Iglesia, E.; Baumgartner, J. E.; Price, G. L. *J. Catal.* **1992**, *134*, 549−571.
(18) Guisnet, M.; Gnep, N. S.; Alario, F. *Appl. Catal., A* **1992**, *89*, 1−30.
(19) Iglesia, E.; Baumgartner, J. E. *Catal. Lett.* **1993**, *21*, 55−70.
(20) Giannetto, G.; Monque, R.; Galiasso, R. *Catal. Rev.—Sci. Eng.* **1994**, *36*, 271−304.
(21) Meriaudeau, P.; Sapaly, G.; Wicker, G.; Naccache, C. *Catal. Lett.* **1994**, *27*, 143−148.
(22) Buckles, G.; Hutchings, G. J. *Catal. Lett.* **1994**, *27*, 361−367.
(23) Guisnet, M.; Gnep, N. S. *Catal. Today* **1996**, *31*, 275−292.
(24) Dooley, K. M.; Price, G. L.; Kanazirev, V. I.; Hart, V. I. *Catal. Today* **1996**, *31*, 305−315.
(25) Nakamura, I.; Fujimoto, K. *Catal. Today* **1996**, *31*, 335−344.
(26) Choudhary, V. R.; Devadas, P. *Appl. Catal., A* **1998**, *168*, 187−200.
(27) Mole, T.; Anderson, J. R.; Creer, G. *Appl. Catal.* **1985**, *17*, 141−154.
(28) Scurrell, M. S. *Appl. Catal.* **1988**, *41*, 89−98.
(29) Ono, Y.; Kanae, K. *J. Chem. Soc., Faraday Trans.* **1991**, *87*, 669−675.
(30) Dufresne, L. A.; Levanmao, R. *Catal. Lett.* **1994**, *25*, 371−383.
(31) Biscardi, J. A.; Iglesia, E. *Catal. Today* **1996**, *31*, 207−231.
(32) Berndt, H.; Lietz, G.; Lucke, B.; Volter, J. *Appl. Catal., A* **1996**, *146*, 351−363.
(33) Kwak, B. S.; Sachtler, W. M. H. *Korean J. Chem. Eng.* **1996**, *13*, 356−363.
(34) Biscardi, J. A.; Iglesia, E. *J. Catal.* **1999**, *182*, 117−128.
(35) Scurrell, M. S. *Appl. Catal.* **1987**, *32*, 1−22.
(36) Kwak, B. S.; Sachtler, W. M. H.; Haag, W. O. *J. Catal.* **1994**, *149*, 465−473.
(37) Mroczek, U.; Steinberg, K. H.; Roessner, F. *React. Kinet. Catal. Lett.* **1991**, *44*, 201−207.
(38) Steinberg, K. H.; Mroczek, U.; Roessner, F. *Appl. Catal.* **1990**, *66*, 37−44.
(39) Gnep, N. S.; Doyemet, J. Y.; Seco, A. M.; Ribeiro, F. R.; Guisnet, M. *Appl. Catal.* **1987**, *35*, 93−108.
(40) Inui, T.; Okazumi, F. *J. Catal.* **1984**, *90*, 366−367.
(41) Meriaudeau, P.; Naccache, C. *Catal. Rev.—Sci. Eng.* **1997**, *39*, 5−48.
(42) Meriaudeau, P.; Naccache, C. *J. Mol. Catal.* **1989**, *50*, L7−L10.
(43) Olah, G. A. *Angew. Chem., Int. Ed. Engl.* **1973**, *12*, 173−254.
(44) Olah, G. A. *J. Org. Chem.* **2001**, *66*, 5943−5957.
(45) Saunders, M.; Jimenez-Vazquez, H. A. *Chem. Rev. (Washington, D.C.)* **1991**, *91*, 375−97.
(46) Olah, G. A.; Surya Prakash, G. K.; Sommer, J. *Superacids*, 1st ed.; John Wiley & Sons: New York, 1985.
(47) Saunders, M.; Vogel, P.; Hagen, E. L.; Rosenfeld, J. *Acc. Chem. Res.* **1973**, *6*, 53−59.
(48) Botkin, J. H.; Forsyth, D. A.; Sardella, D. J. *J. Am. Chem. Soc.* **1986**, *108*, 2797−2802.
(49) Franke, W.; Schwarz, H.; Thies, H.; Chandrasekhar, J.; Schleyer, P. v. R.; Hehre, W. J.; Saunders, M.; Walker, G. *Angew. Chem.* **1980**, *92*, 488−90.
(50) Saunders, M.; Berger, R. *J. Am. Chem. Soc.* **1972**, *94*, 4049−50.
(51) Saunders, M.; Kates, M. R. *J. Am. Chem. Soc.* **1978**, *100*, 7082−3.
(52) Cavallotti, C.; Rota, R.; Carra, S. *J. Phys. Chem. A* **2002**, *106*, 7769−7778.
(53) Dubnikova, F.; Lifshitz, A. *J. Phys. Chem. A* **2002**, *106*, 8173−8183.
(54) Madden, L. K.; Mebel, A. M.; Lin, M. C.; Melius, C. F. *J. Phys. Org. Chem.* **1996**, *9*, 801−810.
(55) Viruela-martin, P. M.; Nebot, I.; Viruelamartin, R.; Planelles, J. *J. Chem. Soc., Perkin Trans. 2* **1986**, 49−53.
(56) Vrcek, V.; Saunders, M.; Kronja, O. *J. Org. Chem.* **2003**, *68*, 1859−1866.
(57) Jenson, C.; Jorgensen, W. L. *J. Am. Chem. Soc.* **1997**, *119*, 10846−10854.
(58) Becke, A. D. *J. Chem. Phys.* **1993**, *98*, 5648−5652.

(59) Krishnan, R.; Binkley, J. S.; Seeger, R.; Pople, J. A. *J. Chem. Phys.* **1980**, *72*, 650−654.
(60) Frisch, M. J.; Trucks, G. W.; Schlegel, H. B.; Scuseria, G. E.; Robb, M. A.; Cheeseman, J. R.; Zakrzewski, V. G.; Montgomery, J. A., Jr.; Stratmann, R. E.; Burant, J. C.; Dapprich, S.; Millam, J. M.; Daniels, A. D.; Kudin, K. N.; Strain, M. C.; Farkas, O.; Tomasi, J.; Barone, V.; Cossi, M.; Cammi, R.; Mennucci, B.; Pomelli, C.; Adamo, C.; Clifford, S.; Ochterski, J.; Petersson, G. A.; Ayala, P. Y.; Cui, Q.; Morokuma, K.; Malick, D. K.; Rabuck, A. D.; Raghavachari, K.; Foresman, J. B.; Cioslowski, J.; Ortiz, J. V.; Stefanov, B. B.; Liu, G.; Liashenko, A.; Piskorz, P.; Komaromi, I.; Gomperts, R.; Martin, R. L.; Fox, D. J.; Keith, T.; Al-Laham, M. A.; Peng, C. Y.; Nanayakkara, A.; Gonzalez, C.; Challacombe, M.; Gill, P. M. W.; Johnson, B. G.; Chen, W.; Wong, M. W.; Andres, J. L.; Head-Gordon, M.; Replogle, E. S.; Pople, J. A. *Gaussian 98*, revision A.7; Gaussian, Inc.: Pittsburgh, PA, 1998.
(61) Davidson, E. R.; Feller, D. *Chem. Rev.* **1986**, *86*, 681−696.
(62) Peng, C. Y.; Ayala, P. Y.; Schlegel, H. B.; Frisch, M. J. *J. Comput. Chem.* **1996**, *17*, 49−56.
(63) Saunders, M.; Rosenfeld, J. *J. Am. Chem. Soc.* **1969**, *91*, 7756−7758.
(64) Kazansky, V. B. *Acc. Chem. Res.* **1991**, *24*, 379−383.
(65) Rigby, A. M.; Kramer, G. J.; van Santen, R. A. *J. Catal.* **1997**, *170*, 1−10.
(66) Kazansky, V. B. *Catal. Today* **1999**, *51*, 419−434.
(67) Rozanska, X.; Demuth, T.; Hutschka, F.; Hafner, J.; van Santen, R. A. *J. Phys. Chem. B* **2002**, *106*, 3248−3254.
(68) Sinclair, P. E.; de Vries, A.; Sherwood, P.; Catlow, C. R. A.; van Santen, R. A. *J. Chem. Soc., Faraday Trans.* **1998**, *94*, 3401−3408.
(69) Bhan, A.; Joshi, Y. V.; Delgass, W. N.; Thomson, K. T. *J. Phys. Chem. B* **2003**, *107*, 10476−10487.
(70) Koningsveld, H. V.; Bekkum, H. V.; Jansen, J. C. *Acta Crystallogr., Sect. B* **1987**, *43*, 127−132.